Beynəlxalq Konfrans "Fizika-2005"
International Conference "Fizika-2005"
Международная Конференция "Fizika-2005"

7 - 9 İyun / June / Июнь 2005 — №210 — səhifə / page / стр. 800-803

Bakı, Azərbaycan — Baku, Azerbaijan — Баку, Азербайджан

OPTICAL CHARACTERIZATION OF WIDE-GAP BIAXIAL $CaGa_2S_4$ BY SPECTROSCOPIC ELLIPSOMETRY AND POLARIZED TRANSMISSION INTENSITIES

YONGGU SHIM[1)] AND NAZIM MAMEDOV[2)]

[1)]Department of Physics and Electronics, Graduate School of Engineering,
Osaka Prefecture University,
Gakuen-cho 1-1, Sakai, Osaka 599-8531, Japan
e-mail: shim@pe.osakafu-u.ac.jp
Phone: +81-72-252-1161(Ext.2399)
Fax: +81-72-254-9908

[2)]Institute of Physics, National Academy of Sciences of Azerbaijan,
Javid ave. 33, Baku, AZ-1143, Azerbaijan

Differently prepared natural (100)-oriented cleavage planes of the orthorhombic wide-gap (E_o~4.1eV) single crystalline $CaGa_2S_4$ were examined in two symmetric positions at room temperature over the photon energies 0.8-6.5eV by spectroscopic ellipsometry. Complimentary, polarized transmission intensity technique was applied. The data obtained by both techniques were further treated within standard biaxial approach and the major refraction indices were restored for the practically important range below energy gap. The structure and polarization peculiarities of the obtained pseudo-dielectric function were related with apparently four critical points of interband electronic transitions in ZZ (E_1=4.49eV, E_3=5.34eV) and YY (E_2=5.00eV, E_4=6.21eV) configurations, respectively.

1. INTRODUCTION

Orthorhombic wide-gap ternary semiconductor $CaGa_2S_4$ (CGS) is regarded as promising host to rare earth Ce and Eu to apply in flat panel displays and lasers [1-3]. For such applications, the photon energy of the utilized light lies in visible blue-to-red or infrared spectral range, being lower than energy gap (~4.10eV [4]) of the material. Growth technique of the single crystalline CGS, which is required for efficient lasers in the first place [2], is now progressing and the samples with large (100) natural cleavage plane are readily available [5]. At the same time, sufficiently large surfaces with other orientation are still a problem.

In view of the above applications, the information on optical constants of single crystalline CGS, especially that for the photon energy range below energy gap is highly required. But, until now there have been no relevant works treating the matter, except for the recently made brief report [6] based on the polarized transmission intensity (PTI) data that can provide only the effective values of optical constants.

Here we give the results of more extended investigation that we performed with the aid of the spectroscopic phase-modulated ellipsometry (SPME) and PTI techniques, by examining CGS samples with (100) surfaces prepared in different ways.

2. EXPERIMENTAL DETAILS

As CGS is a biaxial, orthorhombic crystal (space group Fddd [7]), it has 3 refraction and 3 extinction coefficients, which are supposed to be determined using conventional biaxial ellipsometry technique. But, ellipsometric determination of all of these unknown parameters is a problem that is difficult to solve using only one crystallographic plane, in particular, the (100) surface mentioned above. Therefore, at this initial stage our strategy was going trough possibly accurate determination of the optical constants of the single crystalline CGS in the practically important photon energy range below energy gap, for which besides ellipsometric parameters (ψ and Δ), PTI spectra were also available. Afterwards both were treated using standard biaxial two-phase model [8,9].

At the photon energies above energy gap, we were using an isotropic two-phase approximation to treat the ellipsometric data obtained in so-called highly symmetric configurations. Information of the energy position and polarization of the structures of the pseudo dielectric function (PDF) obtained in such configurations is believed to be close to real [10].

Two symmetric sample positions regarding the plane of incidence were determined by using a special rotation stage mounted on a Jobin-Yvon spectroscopic phase-modulated ellipsometer UVISEL-9017TK whose photon energy range (0.75eV to 6.50eV) was wide enough to comprise both energy regions, such as above and below energy gap of CGS. The last region was also examined by using a PTI technique described previously [11]. All measurements were done at room temperature in the air ambience.

3. RESULTS AND DISCUSSION

3.1 Overlayer and PDF

As explained in the previous section, the two-phase model was the most preferable option and we were trying to find adequate sample surfaces by preparing them in different ways and monitoring the effect on ellipsometric parameters. In our evaluations, we were relaying upon the fact that for the perfect case in the region below energy gap, parameter Δ should assume ether 0^o or 180^o value since absorption is negligible.

For a period of the SPME measurements carried out immediately after cleaving we can probably ignore oxidization or contamination process that certainly occurred on the (100) surface, with a noticeable effect on Δ (and ψ) at the sufficiently large time scale. A corresponding remarkable change of PDF, in particular, that of the imaginary part, $\langle\varepsilon_2\rangle$, is shown in Fig.1a where arrows indicate the direction of the shift of the absolute value of $\langle\varepsilon_2\rangle$ towards higher or lower values in the accessed spectral range in certain time-intervals after cleaving. The data are given for a configuration (ZZ) for which the plane of the incident light is parallel to Z crystal axis lying in the (100) surface plane.

An oxidization or contamination related overlayer that was growing with longer exposition of samples to air is behind the observed picture with an upward shift at the photon energies lower than ~ 4.9eV and a downward shift at the higher energies.

On the other hand, a roughness-related overlayer also leads to similar shifts in exactly the same energy ranges, as seen from Fig.1b where $\langle\varepsilon_2\rangle$ is shown for CGS after different periods of etching in $HCl:H_2O$ solution with ingredients taken in proportion 1:100, respectively. (A significant increase of the roughness of the examined surface after increasing etching time was solidly verified by observations with a high-grade optical microscope.)

Thus, oxidization (or surface contamination) and surface roughness eventually produce the similar changes in the spectral shape of $\langle\varepsilon_2\rangle$. Consequently, a criterion such as the larger $\langle\varepsilon_2\rangle$ above 4.9eV and the smaller it is below this energy the better can be conceived and used for the benefit of the two-phase model. The best results according to this criterion are achieved for the natural freshly prepared cleavage planes after a soft mechanical polishing with 0.1μm alumina suspension and consequent washing in the acetone and water and drying.

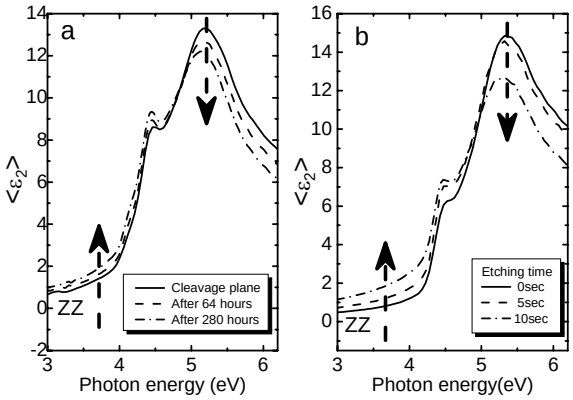

Fig.1 The spectrum of imaginary part of PDF of CGS in certain time-intervals after cleaving (a) and after different periods of etching in $HCl:H_2O$ (1:100) solution (b). Vertical arrows indicate the direction of the shift of the amplitude of $\langle\varepsilon_2\rangle$ towards higher or lower values in the accessed spectral range

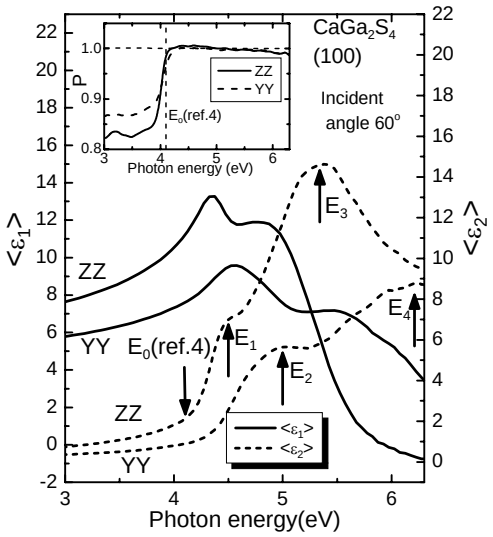

Fig.2 Spectra of real ($\langle\varepsilon_1\rangle$) and imaginary ($\langle\varepsilon_2\rangle$) parts of pseudo-dielectric function of CGS for configurations ZZ and YY. Arrows show energy positions of the structures of $\langle\varepsilon_2\rangle$. Inset: photon energy dependence of polarization degree of the light reflected by a 125μm thick CGS.

Both real and imaginary parts of PDF obtained under the just-mentioned conditions are shown in Fig.2 separately for YY and ZZ configurations.

Four oscillator-type peculiarities with peak-like structures in $\langle\varepsilon_2\rangle$ are clearly seen. The last structures are denoted as E_1=4.49eV, E_3=5.34eV and E_2=5.00eV, E_4=6.21eV for ZZ and YY components of PDF, respectively. Apparently, these peculiarities are related with the critical points of interband density of states. However this point is a matter for further extended analyses beyond the frames of the present work. As to

band gap singularity, E_o in Fig.2, its reported position (~4.1eV [4]) is indeed within the range of energies of a sharp change of polarization degree (see inset) for a relevantly thick CGS sample, i.e. as expected for a transition from coherent to incoherent reflection near the absorption edge [12].

3.2 Optimized refraction indices

The earlier reported large effective value of birefringence in (100) plane [6] in the region below energy gap is certainly related with strong anisotropy of dielectric function of CGS, which was clearly displayed by PDF shown above. For more confidence, here we give the effective values of all major refraction indices that were obtained from the interference fringes in PTI spectra taken in relevant configurations. These values were then fitted to the Sellmeier's dispersion model with oscillator energies taken to be equal with the energies of the above critical points.

The obtained effective values of n_y and n_z are given by open circles while fitting results by solid lines in Fig.3. Relevant fringe picture is shown in inset. The third index, n_x, which was obtained at inclined incidence, is given by square dots in Fig.3. In spite of poor accuracy (±0.1) of determination of the last index, we believe that it was smaller than n_z or n_y at least for the wavelengths ranging from 520nm to 750nm.

As mentioned, the data in Fig.3 represent only effective values of refraction indices. On account of the dispersion effect these values may need some correction, which can be done by comparison with ellipsometric results.

At the photon energies below energy gap extinction can be ignored and the complex ellipsometric ratio ρ given in biaxial formulation [9] as

$$\rho_{z(y)} = \frac{n_{z(y)} n_x \cos\varphi - \sqrt{n_x^2 - \sin^2\varphi}}{n_{z(y)} n_x \cos\varphi + \sqrt{n_x^2 - \sin^2\varphi}} \times \frac{\cos\varphi + \sqrt{n_{y(z)}^2 - \sin^2\varphi}}{\cos\varphi - \sqrt{n_{y(z)}^2 - \sin^2\varphi}} \qquad (1)$$

where z is taken for the configuration Z-axis || incidence plane and y for Y-axis || incidence plane, both axes in the (100) plane, becomes real. In this case, the ellipsometric equations can be rewritten to the form

$$\rho_z = \tan\psi_z,\ \rho_y = \tan\psi_y \qquad (2)$$

with the same meaning of z and y as before. By minimizing error function [13] rewritten to the form

$$G(n_x, n_y, n_z) = \sum_{\delta} (\rho_\delta^{meas} - \rho_\delta^{calc})^2 \qquad (3)$$

where ρ_δ^{meas} is the relative reflection coefficient measured in configuration δ (z or y), and ρ_δ^{calc} is the one calculated according to equations (1), we can find all major refraction indices with a certain degree of confidence depending on the convergence of the obtained results.

The optimized refraction indices that were found after application of an iteration procedure to solve equations (1) and (2) and to minimize error function (3) are shown in Fig.4.

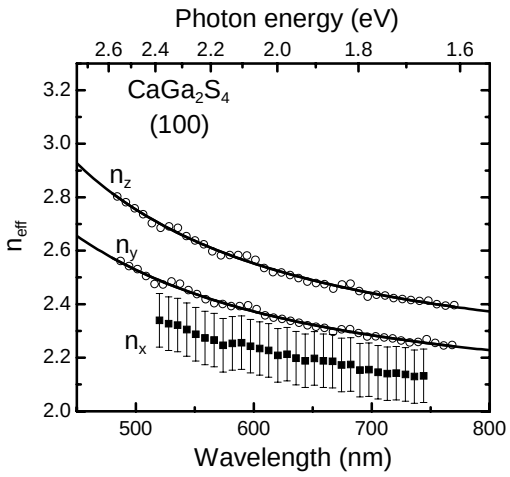

Fig.3 Effective values of major refraction indices as obtained from PTI data (see text for explanations). Inset: PTI-spectra of a 128μm thick CGS for different orientations.

The results for refraction indices n_y and n_z, which are respectively given by open squares and circles in Fig.4, display good convergence within the indicated error bars. The results for n_x, however, are dependent of starting parameters of iteration within much wider margins. The dashed curve in Fig.4 represents the most probable scenario of the wavelength dependence of this index that is apparently crossing n_y and n_z in the short wavelength spectral range.

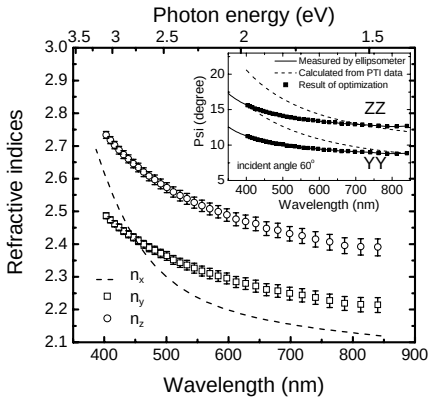

Fig.4 Wavelength dependence of optimized refraction indices of CGS. Inset: Wavelength dependence of amplitude diminution as obtained from experiment (solid line) and calculations using effective (dashed line) and optimized (squares) refraction indices.

Using just-mentioned major refraction indices, a good reproducibility of ψ in the region below energy gap (Δ is 0) is feasible. An example is shown in inset of Fig.4. As expected, the difference between ellipsometric and PTI results is growing with decreasing wavelength and approaching absorption edge. In the long wavelength spectral range ellipsometric and PTI results are essentially the same.

4. CONCLUSIONS

We have carried out SPME and PTI studies on single crystalline CGS samples with differently prepared (100) surfaces and obtained, for the first time, information of the major refraction indices of this biaxial material in the practically important region below energy gap. We have also found that PDF of CGS is very anisotropic and this anisotropy apparently originates from the different critical points forming ZZ and YY tensor components of dielectric function. Because of the accuracy related problems, the further progress of ellipsometric characterization of biaxial CGS is dependent of availability of the (010) or (001) surfaces of a good optical quality that is essential for justifiable application of the two-phase model to this material, which is new from the optical point of view and any surface related problem would be a very undesirable obstacle.

A part of the samples we used in the present work was kindly provided by Prof. T. Takizawa and Dr. C. Hidaka, for which we are very grateful. We thank Mr. S. Kondo and M. Yasuoka for technical assistance in some experimental procedures. This research was partially supported by the Ministry of Education, Culture, Sports, Science and Technology, Japan, Grant-in-Aid for Young Scientists (B), 15760008, 2005.

[1]. K. Tanaka, Y. Inoue, S. Okamoto, K. Kobayashi and K. Takizawa, Jpn. J. Appl. Phys. 36 (1997) 3515.

[2]. S. Iida, T. Matsumoto-Aoki, T. Morita, N. Mamedov, B. G. Tagiev, F. M. Gashimzade and K. Sato, Jpn. J. Appl. Phys. Suppl. 39-1 (2000) 429.

[3]. M. C. Nostrand, R. H. Page, S. A. Payne, W. F. Krupke and P. G. Schunemann, Opt. Lett. 24 (1999) 1215.

[4]. N. Mamedov, H. Toyota, A. Yasunaka, Y. Shim, A. Kato, A. Ashida, S. Iida and N. Yamamoto, Phys. Stat. Sol. (a) 198 (2003) 478.

[5]. C. Komatsu and T. Takizawa, J. Cryst. Growth 222-3 (2001) 574.

[6]. Y. Shim, N. Mamedov, N. Yamamoto, J. Phys. Chem. Solids 64 (2003) 1811.

[7]. B. Eisenmann, M. Jakowski, W. Klee, H. Shäfer, Revue de Chimie minérale 20 (1983) 225 (in German).

[8]. R. M. A. Azzam, N. M. Bashara, Ellipsometry and Polarized Light, Elsebier, Amsterdam, 1986.

[9]. R. H. W. Graves, J. Opt. Soc. Am. 59 (1969) 1225.

[10]. D. E. Aspnes, J. Opt. Soc. Am. 70 (1980) 1275.

[11]. N. Mamedov, Y. Shim, N. Yamamoto, Jpn. J. Appl. Phys. 41 (2002) 7254.

[12]. M. Kildemo, R. Ossikovski, M. Stchakovsky, Thin Sold Films 313-314 (1998) 108.

[13]. S. Logothetidis, M. Cardona, P. Lautenschlager, M. Garriga, Phys. Rev. B 34 (1986) 2458.